

# New Target of Oxidative Stress Regulation in Cochlea: Alternative Splicing of the p62/Sqstm1 gene

**Pengjun Li**

Zhejiang University

**Dan Bing**

Tongji Medical College of Huazhong University of Science and Technology; Huazhong University of Science and Technology Tongji Medical College

**Xiaodi Wang**

Tongji Medical College of Huazhong University of Science and Technology; Huazhong University of Science and Technology Tongji Medical College

**Jin Chen**

Tongji Medical College of Huazhong University of Science and Technology; Huazhong University of Science and Technology Tongji Medical College

**Zhihui Du**

Tongji Medical College of Huazhong University of Science and Technology; Huazhong University of Science and Technology Tongji Medical College

**Yanbo Sun**

Tongji Medical College of Huazhong University of Science and Technology; Huazhong University of Science and Technology Tongji Medical College

**Fan Qi**

Tongji Medical College of Huazhong University of Science and Technology; Huazhong University of Science and Technology Tongji Medical College

**Hanqi Chu** (✉ [qi7chu@163.com](mailto:qi7chu@163.com))

Tongji Hospital of Tongji Medical College of Huazhong University of Science and Technology  
<https://orcid.org/0000-0003-0977-622X>

---

## Research Article

**Keywords:** age-related hearing loss, noise-induced hearing loss, oxidative stress, Nrf2, alternative splicing of the p62 gene

**Posted Date:** May 24th, 2021

**DOI:** <https://doi.org/10.21203/rs.3.rs-535219/v1>

**License:**  This work is licensed under a Creative Commons Attribution 4.0 International License.

[Read Full License](#)

---

# Abstract

To examine the oxidative stress and the antioxidant response of p62-Keap1-Nrf2 pathway in cochleae during age-related hearing loss (ARHL) and noise-induced hearing loss (NIHL), and then elucidate the function of full-length and variant p62/Sqstm1 (referred to here as p62) in the regulation of Nrf2 activation. Cochlear damage was assessed by analyzing auditory brainstem response (ABR) and by counting hair cells (HCs). For oxidative stress detection, the malondialdehyde (MDA) levels and 7, 8-dihydro-8-oxoguanine (8-oxoG) expression in the cochleae was measured by assay kits and immunohistochemistry, respectively. The expression of full-length and variant p62 in cochleae, hippocampus (HIP) and auditory cortex (AC) was found by western blotting; For the Keap1-Nrf2 pathway activation, the Nrf2 nuclear translocation and the Nrf2 target genes HO-1/NQO-1 expression was detected by western blotting and qRT-PCR, respectively. The oxidative function of full-length and variant p62 was examined in HEI-OC-1 cells by flow cytometry. The results showed hearing loss and cochlear hair cell loss was associated with MDA accumulation and 8-oxoG expression during ARHL and NIHL. Nrf2 showed no obvious changes in nuclear protein. Expression levels mRNA for HO-1 and NQO1 was lower in old mice and mildly greater in AT Mice. The expression of p62 splicing variant lacking the Keap1-interacting region was greater than full-length p62 in cochleae. However, the expression of p62 splicing variant was lesser than full-length p62 in HIP and AC. For HEI-OC-1 cells, high expression of full-length p62 decreased ROS levels induced by H<sub>2</sub>O<sub>2</sub>. Oxidative stress is closely related to ARHL and NIHL. Changing the ratio of full-length to variant p62 protein expression may be a new target to reduce the level of oxidative stress in cochleae.

## 1. Introduction

Age-related hearing loss (ARHL) and noise-induced hearing loss (NIHL) are two major classes of sensorineural hearing loss. Among the primary pathological changes of ARHL and NIHL is irreversible loss of sensory cells (Frisina 2009; Li et al. 2019). Studies demonstrated that the imbalance of redox regulation in ARHL and NIHL cause sensory cell loss (Menardo et al. 2012; Honkura et al. 2016). It is plausible that regulation of redox reactions and inhibition of the production of reactive oxygen species (ROS) may help prevent sensory cell damage.

The p62-Keap1-Nrf2 pathway is a major mechanism in regulation of cellular redox homeostasis (Chen et al. 2009; Harder et al. 2015; Pan et al. 2016). p62 is a stress-induced cellular protein that possesses several regions that mediate its interactions with other proteins to regulate cellular mechanisms such as autophagy, ubiquitination, and apoptosis (Bjorkoy et al. 2005; Katsuragi et al. 2015; Wang et al. 2017). In response to oxidative stress, p62 forms a homodimer via the K7-D69 hydrogen bond in its Phox1 and Bem1p (PB1) domains (Wilson et al. 2003). This process facilitates p62 oligomerization and interaction with Keap1 via its Keap1-interacting region (KIR) (Komatsu et al. 2010; Lau et al. 2010). Thereby causing Nrf2 stabilization and activation. In the nucleus, Nrf2 binds to the antioxidant response element located in DNA to activate antioxidant genes such as HO-1, Nqo-1, Gclc, and Gclm (Kobayashi et al. 2004; Honkura et al. 2016; Fetoni et al. 2019). P62 gene is also the target of Nrf2, and the nuclear translocation

of Nrf2 promotes the expression of p62 protein (Jain et al. 2010; Kageyama et al. 2018). These findings suggest that there is a positive feedback loop in the p62-Keap1-Nrf2 axis.

In the human cochleae, Nrf2 is predominantly expressed in the organ of Corti and is seldomly expressed in the spiral ligament, stria vascularis, or Reissner's membrane (Hosokawa et al. 2018). The neurons of the spiral ganglia are almost devoid of Nrf2. The organ of Corti and especially its hair cells are susceptible to production of ROS. In animals, studies suggested that Nrf2 activation protects the inner ear from age- and ototoxic drug-related injuries (Kong et al. 2009; Hoshino et al. 2011; Kim et al. 2015). Similarly, drug-induced Nrf2 activation protects hair cells from ROS-related damage induced by overexposure to noise (Fetoni et al. 2015; Honkura et al. 2016). However, antioxidant gene expression regulated by Nrf2 barely increases after pure noise exposure (Honkura et al. 2016; Xiong et al. 2019). This indicates that ROS induced by noise exposure may not effectively activate the Nrf2 pathway under physiological conditions.

In the present study, we investigated whether noise- and age-related cochlear injuries activated the p62-Keap1-Nrf2 pathway in C57BL/6 mice. We also measured the expression of splicing variants and full-length p62 in the cochlea and other tissue. We then carried out experiments in HEI-OC-1 cells to elucidate the role of full-length or variant p62 in the regulation of Nrf2 activation.

## **2. Materials And Methods**

### **2.1. Animals and Anesthesia**

Male C57BL/6 mice were used for in vivo studies. The mice were divided into five groups, as follows: young group (51 mice, 2 months old), old group (51 mice, 13–14 months old), control group (56 mice, 2 months old), acoustic trauma (AT) group (58 mice, 2 months old), and TBHQ injection group (10 mice, 2 months old). The mice were purchased from Beijing Vital River Laboratory Animal Technology Co., Ltd. Care of the animals and experimental protocols were approved by the Animal Research and Ethics Committee of Tongji Medical College, Huazhong University of Science and Technology, China.

Before conducting the hearing measurements and acoustic overexposures, the mice were anesthetized with chlorpromazine hydrochloride 20 mg/kg body weight (Harvest Pharmaceutical Co., Ltd., Shanghai, China) and ketamine hydrochloride 120 mg/kg body weight (Gutian Pharma Co., Ltd., Fujian, China).

### **2.2. Acoustic Overexposure**

Mice were exposed to broad band noise (8–16 kHz) under anesthesia at 105 dB SPL for 2 h. The entire device was placed in a small, reverberant chamber. Noise was played over the horn. Noise calibration was performed before exposure where the noise level difference in each compartment was less than 1 dB.

### **2.3. Assessment of Auditory Function**

Hearing threshold was assessed using click- and tone burst- auditory brainstem response (ABR) recordings. The TDT system III (Tucker-Davis Technologies, Alachua, FL, USA) was used to generate stimulus and record trigger signal. Generated tone burst stimuli were delivered at 8, 16, 24, and 32 kHz into the external auditory canal of the mice through an electrostatic speaker placed close to the head. Evoked potentials were filtered between 100 and 3000 Hz using the TDT system and the averages were noted 512 times. The highest stimulus intensity used was 90 dB with a sequential decrease by 10 dB until we identified the lowest sound level able to elicit a repeatable wave sufficient to be considered the threshold. The number of mice undergoing ABR testing included 13 mice in the young group, 13 in the old group, 8 in the control group, and 10 mice in the AT group. For the young and old groups, we performed ABR testing once. For the control and AT groups, we tested ABR thresholds at baseline (pre-AT) and 2 weeks after AT (post-2w); Threshold shift = threshold (post-2w) – threshold (pre-AT).

## 2.4. TBHQ Administration

TBHQ is a widely used Nrf2 activator that promotes Nrf2 for its nuclear translocation and its antioxidant activation. TBHQ was obtained from MedChemExpress (Monmouth Junction, NJ, USA). TBHQ solution was intraperitoneally injected at 50 mg/Kg. The injection was administered 12 h before sacrifice and tissue preparation. Ten mice were used for TBHQ injection.

## 2.5. Cell Cultures and H<sub>2</sub>O<sub>2</sub> Administration

HEI-OC-1 cells were cultured at 33 °C with 10% CO<sub>2</sub> in DMEM media containing 1.0 g/L glucose and 10% FBS. For plasmid construction, the CDS of full-length or variant p62 with 3 × flag was separately cloned into a pcDNA3.1 + plasmid to create transients overexpressing various transcripts of the p62 gene. The pcDNA3.1+/vector was used as control. HEI-OC-1 cells were treated with H<sub>2</sub>O<sub>2</sub> (200 mM) for 24 h, after which cells were collected for ROS detection.

## 2.6. Immunohistochemistry

Immunohistochemistry was used to determine levels of 7, 8-dihydro-8-oxoguanine (8-oxoG), a key biomarker of mitochondrial and nuclear DNA oxidative stress damage. Three mice per group underwent 8-oxoG testing. Mice were decapitated 6 h after acoustic overexposure. Cochleae were isolated, followed by immersion fixation in 4% paraformaldehyde overnight. Decalcification using 10% sodium EDTA was then performed for 2 days followed by overnight incubation in Hanks buffered saline with 25% sucrose. Cochleae were embedded in optimal cutting temperature compound, cryosectioned at 10 μm thickness, mounted on microscope slides, and stored at – 20°C. Slides with cochlear tissues were dried at room temperature for 30 min. Slides were then permeabilized for 10 min using 0.3% Triton X-100/PBS, washed with PBS and blocked for 60 min using 10% goat serum/PBS. Finally, slides were incubated overnight with primary antibodies (mouse monoclonal anti-8oxoG-DNA lesion; 1:100; Santa Cruz, Santa Cruz, CA, USA) diluted in 0.5% BSA/PBS at 4 °C. On the following day, slides were washed with PBS and incubated for 1 h with secondary antibody (1:400; GAR4882, Multi sciences, Hangzhou, China). After washing twice, the nuclei were dyed with DAPI (G1012, Servicebio, Wuhan, China) followed by observation under a fluorescence microscope (400×).

For outer hair cell counting, mice were decapitated 2 weeks after acoustic overexposure. Three mice from each group underwent outer hair cell counting. Cochleae were isolated, followed by fixation. Basal turn membranes were then carefully dissected, followed by permeation for 10 min with 0.3% Triton X-100/PBS and dyed using DAPI. Finally, they were observed under a fluorescence microscope (400×).

## 2.7. Immunoblotting

Some of the animals of the AT and control groups were decapitated 6 h after acoustic overexposure or sham exposure. Other groups of mice were decapitated directly. Immediately after that, the cochleae were dissected, followed by immersion in cold PBS, and then whole cochlear tissue with bone removed was collected for immunoblotting. The hippocampus (HIP) and auditory cortex (AC) were washed in PBS, dissected, and collected on ice.

Expression levels of p62 were measured using total protein of cochleae, HIP, and AC. Tissues were homogenized using RIPA lysis buffer (G2002, Servicebio) including protease inhibitors and phenylmethanesulfonyl fluoride (PMSF) cocktail (G2008, Servicebio). Decomposition using ultrasound was followed by 30 min standing on ice. Total protein was finally collected by centrifugation and protein concentrations were measured using a bicinchoninic acid kit (G2026, Servicebio). Nuclear proteins collected from the cochleae were used to measure Nrf2 nuclear translocation. Nuclear protein extraction was performed using a nuclear and cytoplasmic protein extraction kit (P150, Promoter Biological, Wuhan, China). Proteins were separated using SDS-PAGE gel and were then transferred to PVDF membranes. Membranes were blocked for 1 h using 3% BSA/TBST, and were then incubated overnight with primary antibodies, p62 (1:1000; ab91526, Abcam, Cambridge, UK), Nrf2 (1:1000; ab62352, Abcam), Lamin B1 (1:500; sc-374015, Santa Cruz), and beta-actin (1:1000, GB11001, Servicebio). On the following day, membranes were washed with TBST and incubated for 1 h with HRP-labeled Goat Anti-Rabbit IgG (GB23033, Servicebio). Membranes were washed again and immersed in electrochemiluminescence solution (ECL, G2020, Servicebio) followed by exposure under an E-Gel Imager.

## 2.8. MDA Assay

Malondialdehyde (MDA) is a lipid peroxidation product. MDA levels in cochleae were measured using an MDA assay kit (Nanjing Jiancheng Bioengineering Institute, Catalog No. A003-1), and the experimental methods were carried out according to the manufacturer's instructions.

## 2.9. Quantitative Real-Time Polymerase Chain Reaction (qRT-PCR)

Dissections of cochleae were followed by immersion in cold PBS and then collection of whole cochlear tissue with bone removed for qRT-PCR. Total RNA was isolated using TRIzol (Invitrogen, Carlsbad, USA), and 1 µg of the extracted total RNA was reverse-transcribed to cDNA following the protocol of ReverTra Ace (Toyobo, Osaka, Japan). Amplification of cDNA samples was performed on a LightCycler 480 II (Roche, Rotkreuz, Switzerland) using SYBR Green Premix Ex Taq™ (Tli RNase H Plus; TaKaRa, Dalian, China). Cycling parameters were 3 min at 95°C, followed by 40 cycles for 15 s at 95°C, 1 min at 60°C, and

30 s at 72°C. Each sample was amplified three times followed by calculation of the mean value. Relative mRNA levels of NQO1 and HO-1 were normalized to GAPDH using the 2<sup>(-Delta Delta CT)</sup> method. The primers used in the present study are displayed in Table 1.

Table 1  
The primers used in the present study.

primer	sequence
HO-1 forward	AAGCCGAGAATGCTGAGTTC
HO-1 reverse	GCCGTGTAGATATGGTACAAGGA
NQO1 forward	TGGCCGAACACAAGAAGC
NQO1 reverse	TGAATCGGCCAGAGAATGAC
p62 forward	GAACATGGAGGGAAGAGAAG
p62 reverse	TCACAATGGTGGAGGGTGCTTCG
beta-actin forward	GGCTGTATTCCCCTCCATCG
beta-actin reverse	CCAGTTGGTAACAATGCCATGT

## 2.10. Agarose Gel Electrophoresis

We performed 2% agarose gel electrophoresis. The p62 qRT-PCR products from cDNA of cochleae and HEI-OC-1 cells underwent gel electrophoresis to identify their sizes in the presence and absence of the last half of exon 7. After electrophoresis, the gels were exposed under an E-Gel Imager and pictures were analyzed using ImageJ 1.52a.

### 2.11. Flow Cytometry

A Reactive Oxygen Species (ROS) Assay Kit (Beyotime, S0033, Shanghai, China) was used for HEI-OC-1 cell ROS analysis. Cell transfection and H<sub>2</sub>O<sub>2</sub> treatment of HEI-OC-1 cells was followed by trypsinization and collection by centrifugation at 2000 rpm for 5 min. Cells were washed in PBS twice. Cells obtained from one hole of a six-hole plate were resuspended in 500 µl DCFH-DA diluent. The cells were incubated for 20 min at 37 °C in the dark followed by analysis using flow cytometry.

### 2.12. Statistical Analysis

Data were expressed as means ± standard deviation (SD). N signified the number of animals per experimental group. Differences between groups with unpaired data were compared using the Student's t-test. *P*-values was presented as follows: \**P* < 0.05; \*\**P* < 0.01; \*\*\**P* < 0.001; and *n.s.* = not significant.

## 3. Results

### **3.1. Cochlear Hair Cell Loss was Associated with ROS Accumulation in the ARHL Model**

To determine the association between ROS and hearing loss, we examined hearing function, HCs, and MDA levels in mice. ABR testing, an objective electrophysiological test of hearing function, was used to monitor the progression of hearing loss. At all tested frequencies, the average thresholds from old mice were significantly greater than those of young mice (Fig. 1A). These results suggest that old C57BL/6 mice developed significant hearing loss.

To determine whether the functional deficits corresponded to the extent and localization of hair cell loss, cochleae were processed for surface preparations and quantitative hair cells counts after the ABR measurements. In the basal cochlear turn in young mice, surface preparations showed regular outlines with one row of inner hair cells and three rows of outer hair cells (Fig. 1B and D). In the 13–14-month-old mice, nearly 68% loss of hair cells was observed in the basal turn. To determine whether oxidative stress contributed to ARHL, MDA levels were measured in young and old mice. These levels were significantly higher in old cochleae (2.8 nmol/mg) than in young cochleae (1.4 nmol/mg) (Fig. 1C). This was then confirmed using fluorescence microscope analysis of 7, 8-dihydro-8-oxoguanine (8-oxoG). When compared with young cochleae, old mice cochleae exhibited higher density of dot-like 8-oxoG staining in the cytoplasm of sensory hair cells (Fig. 1E).

### **3.2. Cochlear Hair Cell Loss is Associated with Oxidative Stress in the NIHL Model**

We then measured hearing function, HCs, and ROS levels in noise-overexposed mice. At all tested frequencies, the average threshold shifts from AT mice were significantly different from those of control mice (Fig. 2A). These results suggest that acoustic overexposure mice developed significant hearing loss. In the basal cochlear turn in control group mice, there was no significant loss of hair cells (Fig. 2B and D). In the AT group mice, there was nearly a 38% loss of hair cells. AT group mice had significantly higher levels of MDA (4.5 nmol/mg) than did control mice (1.4 nmol/mg) (Fig. 2C). We also found that 8-oxoG was more highly expressed in the noise-exposed group than in the control group (Fig. 2E).

### **3.3. Nrf2 Target Gene Expression was Lower in Old Mice and Mildly Greater in AT Mice**

Nrf2 nuclear translocation was examined in young, old, control, and AT mice using immunoblotting. The positive control (PC) group, which underwent TBHQ administration, showed marked nuclear translocation of Nrf2. By contrast, Nrf2 showed no obvious changes in nuclear protein during aging and noise overexposure (Fig. 3A). Expression levels mRNA for Nrf2 target genes HO-1 and NQO1 were measured using quantitative real-time polymerase chain reaction (qRT-PCR). We found that HO-1 and NQO1 expression became notably lower in the cochleae with aging (Fig. 3B and C). After noise overexposure, we

only saw a slight increase in HO-1 expression levels, while those of NQO1 remained unchanged (Fig. 3D and E).

### **3.4. A p62 Splicing Variant Lacking the Keap1-Interacting Region was Overexpressed in Cochleae**

Two distinct bands were observed in p62 immunoblots. The mRNA sequences of these two proteins were predicted based on previous studies and on the mouse Ensembl database ([http://www.ensembl.org/Mus\\_musculus/Info/Index](http://www.ensembl.org/Mus_musculus/Info/Index)). Figure 4A illustrates the presence of a variant of p62 mRNA in which the last half of exon 7 of the full-length p62 mRNA is omitted. Naturally, the variant encodes a p62 protein that lacks the final half of the KIR (Fig. 4B). Primers were designed to verify existence of the two transcripts of p62 in the cochleae and HEI-OC-1 cells (Fig. 4C). The cDNA of cochleae and HEI-OC-1 cells were amplified using qRT-PCR, and the PCR products were used for gel electrophoresis. We found that the sizes of the PCR products were consistent with the prediction (Fig. 4D).

In cochleae, expression levels of the variant p62 were higher than those of full-length p62, regardless of mouse group (Fig. 4E, F, H, and I). The ratios between the variants and the full-length p62 did not change during aging or noise overexposure (Fig. 4G and J). These findings suggested the presence of a variant of p62 lacking the KIR and that the gene expression mechanism is identical to that of the full-length protein. Expression levels of the variant and the full-length p62 in cochleae increased after noise overexposure. There was no significant difference between the young and old groups. We then compared expression levels of p62 in the HIP and AC with those in the cochleae (Fig. 4K). We found there were substantial differences in the ratio between expression of the variant and the full-length p62. The ratio in cochleae was significantly higher than those of the HIP or AC (Fig. 4L).

### **3.5. High Expression of Full-Length p62 Decreased ROS Levels Induced by H<sub>2</sub>O<sub>2</sub>**

To determine whether transfected cells had high expression levels of full-length and variant p62, we used flag immunoblotting (Fig. 5A). HEI-OC-1 auditory cells were incubated with H<sub>2</sub>O<sub>2</sub> (200 μM) for 24 h to induce oxidative stress injury. Expression levels of Nrf2 target genes were measured after oxidative stress (Fig. 5B and 5C). We found that 200 μM H<sub>2</sub>O<sub>2</sub> did not induce significant expression of antioxidant genes. Similarly, antioxidant gene expression levels in cells transiently overexpressing variant p62 cells did not change after oxidative stress. By contrast, antioxidant gene expression levels were markedly increased after oxidative stress in cells overexpressing full-length p62.

Intracellular ROS levels were determined using flow cytometry (Fig. 5D). We found substantial ROS accumulation after H<sub>2</sub>O<sub>2</sub> treatment (red curve). Similarly, in cells overexpressing the variant p62 combined with H<sub>2</sub>O<sub>2</sub> treatment (H<sub>2</sub>O<sub>2</sub> + variant p62, blue curve), the accumulation of ROS was similar to that seen with H<sub>2</sub>O<sub>2</sub> treatment alone. The accumulation of ROS in cells overexpressing full-length p62

combined with H<sub>2</sub>O<sub>2</sub> treatment (H<sub>2</sub>O<sub>2</sub> + full-length p62, black curve) was less than that of cells treated with H<sub>2</sub>O<sub>2</sub> alone.

## 4. Discussion

We found that hearing loss and hair cells loss is accompanied by increased ROS levels in aging and noise overexposure C57 mice. However, the Nrf2 pathway, an important intracellular antioxidant response pathway, was not activated. We found that a variant p62, a potential negative regulator of the Keap1-Nrf2 pathway, was highly expressed in cochleae. We also found that high expression levels of full-length p62 in HEI-OC-1 cells promoted the activation of Nrf2 pathway, increasing the expression of downstream antioxidant genes, and reducing the cellular levels of ROS. In *vitro*, hair cells were not extracted very accurately for experiments, which was a defect of this experiment. However, Nrf2 was mainly expressed in hair cells and seldomly expressed in other part of cochleae, including spiral ligament, stria vascularis, Reissner's membrane and spiral ganglia (Hosokawa et al. 2018). Therefore, it was more meaningful to discuss Nrf2 and p62 in hair cells.

Oxidative damage causes age-related and noise-induced hearing loss (Fetoni et al. 2015; Honkura et al. 2016). In old mice cochleae, we found an imbalance of redox regulation that was manifested by the expression of 8-oxog and the accumulation of MDA. Expression levels of Keap1-Nrf2 pathway target genes, HO-1 and NQO1, were notably lower in old mice. It is not difficult to understand that the reduction of antioxidant enzymes causes oxidative stress during aging (Menardo et al. 2012). Following noise exposure, the cochleae rapidly underwent significant oxidative damage (Wu et al. 2020). The damage was closely related to HC loss and permanent auditory threshold shifts. We found that the Keap1-Nrf2 pathway in the cochleae was not significantly activated after this acute oxidative damage. However, the agonist of the Nrf2 pathway enhanced the amount of Nrf2 nuclear translocation. This suggests a mechanism in which the antioxidant pathway was difficult to be activated in the context of accumulation of ROS, rather than one in which it could not be activated in the mouse cochlea. These findings suggest that there is a negative regulator of Nrf2 pathway in the cochleae under physiological conditions, and that the Nrf2 pathway plays an important role in antioxidant reactions in the cochleae.

Under normal conditions, upon exposure to oxidative stress, specific cysteine residues of Keap1 are modified by oxidants, and the Keap1 homodimer loses its two-site binding affinity for Nrf2 (Bjorkoy et al. 2005; Rogov et al. 2014). As a result, Nrf2 escapes from the Keap1 interaction and translocates into the nucleus (Komatsu et al. 2010; Pan et al. 2016). And full-length p62 having the KIR region can interact with Keap1 to prevent from trapping Nrf2. However, variant p62 lacking the KIR region results in a negatively regulated Nrf2 pathway (Kageyama et al. 2018). We found that there was highly specific expression of the variant p62 in the cochlea. This may be the reason why ROS was enhanced after noise whereas the Nrf2 pathway was not activated. However, for the cerebral cortex and HIP, the expression of the full-length p62 was more than twice that of the splice variant. Unsurprisingly, Nrf2 pathway was significantly activated after ROS stress in the mouse cerebral cortex and hippocampal cells (Liu et al. 2014; Lee et al. 2016). Despite the expression of p62 increasing after noise overexposure, the ratio of splice variant to

full-length protein remained unchanged. This suggests that the gene expression mechanism of variant p62 lacking the KIR is identical to that of the full-length protein. In vitro experiments confirmed that overexpression of full-length p62 activated the Nrf2 pathway induced by oxidative stress, while the expression of antioxidant genes in wild-type cells did not change after oxidative stress. By contrast, there was no significant decrease in antioxidant gene expression after overexpression of the variant p62. The reason may be that expression levels of endogenous p62 splicing variant were large, and its inhibition for Nrf2 pathway reached a maximum. When the exogenous variant p62 was expressed, inhibition of the Nrf2 pathway was unchanged.

Pre-mRNA splicing resulted in the generation of several products that expanded genomic information (Lau et al. 2010). In exon 7 of mouse p62, there is a typical 5' splicing site that is recognized by a component of the spliceosome, i.e., U1 snRNP. If the site is recognized by U1 snRNP, the mRNA coding the variant is generated. If not, full-length p62 mRNA is generated. This may be the mechanism of the high expression of variant p62 in the cochleae.

## 5. Conclusion

The ROS accumulation is closely related to ARHL and NIHL. The inability of ROS accumulation to activate the Nrf2 antioxidant stress pathway under physiological conditions may be related to the alternative splicing of the p62 mRNA in cochleae. It may be beneficial to protect cochlear hair cells by adjusting alternative splicing of the p62 mRNA to increase the expression of full-length p62 and decrease splice variant. The mechanism of p62 mRNA alternative splicing regulation should be studied further.

## Abbreviations

ARHL, age-related hearing loss; NIHL, noise-induced hearing loss; ROS, reactive oxygen species; ABR, auditory brainstem response; 8-oxoG, 7, 8-dihydro-8-oxoguanine; HIP, hippocampus; AC, auditory cortex; MDA, Malondialdehyde.

## Declarations

### o Ethics approval and consent to participate

Care of the animals and experimental protocols were approved by the Animal Research and Ethics Committee of Tongji Medical College, Huazhong University of Science and Technology, China.

o **Consent for publication:** Consent.

### o Availability of data and materials

The data is available upon request.

### o Competing interests

The authors declare that there are no conflicts of interest regarding the publication of this paper.

### **o Funding**

This work was supported by the National Natural Science Foundation of China (Grant Nos. 81500794, 81771004, and 81500791).

### **o Authors' contributions**

Dan Bing and Hanqi Chu designed and conceived the experiments. Pengjun Li, Xiaodi Zhang, Zhihui Du, Yanbo Sun, and Fan Qi performed the experiments. Pengjun Li wrote the manuscript. Chen Jin performed tissue preparation and immunohistochemistry. Xiaodi Zhang were mainly responsible for cell culture. Dan Bing and Hanqi Chu interpreted the data and revised the manuscript.

### **o Acknowledgements**

Thanks to Hao Xiong for donating HEI-OC-1 cell lines to us.

## **References**

Bjorkoy G, Lamark T, Brech A, Outzen H, Perander M, Overvatn A, Stenmark H, Johansen T (2005) p62/SQSTM1 forms protein aggregates degraded by autophagy and has a protective effect on huntingtin-induced cell death. *J Cell Biol* 171:603-14

Chen W, Sun Z, Wang X, Jiang T, Huang Z, Fang D, Zhang DD (2009) Direct Interaction between Nrf2 and p21Cip1/WAF1 Upregulates the Nrf2-Mediated Antioxidant Response. *Molecular Cell* 34:663-673

Fetoni AR, Paciello F, Rolesi R, Eramo SLM, Mancuso C, Troiani D, Paludetti G (2015) Rosmarinic acid up-regulates the noise-activated Nrf2/HO-1 pathway and protects against noise-induced injury in rat cochlea. *Free radical biology & medicine* 85:269-281

Fetoni AR, Paciello F, Rolesi R, Paludetti G, Troiani D (2019) Targeting dysregulation of redox homeostasis in noise-induced hearing loss: Oxidative stress and ROS signaling. *Free Radical Biology and Medicine* 135:46-59

Frisina RD (2009) Age-related Hearing Loss. *Annals of the New York Academy of Sciences* 1170:708-717

Harder B, Jiang T, Wu T, Tao S, de la Vega MR, Tian W, Chapman E, Zhang DD (2015) Molecular mechanisms of Nrf2 regulation and how these influence chemical modulation for disease intervention. *Biochemical Society Transactions* 43:680-686

Honkura Y, Matsuo H, Murakami S, Sakiyama M, Mizutari K, Shiotani A, Yamamoto M, Morita I, Shinomiya N, Kawase T, Katori Y, Motohashi H (2016) NRF2 Is a Key Target for Prevention of Noise-Induced Hearing Loss by Reducing Oxidative Damage of Cochlea. *Scientific Reports* 6

- Hoshino T, Tabuchi K, Nishimura B, Tanaka S, Nakayama M, Ishii T, Warabi E, Yanagawa T, Shimizu R, Yamamoto M, Hara A (2011) Protective role of Nrf2 in age-related hearing loss and gentamicin ototoxicity. *Biochemical and Biophysical Research Communications* 415:94-98
- Hosokawa K, Hosokawa S, Ishiyama G, Ishiyama A, Lopez IA (2018) Immunohistochemical localization of Nrf2 in the human cochlea. *Brain Research* 1700:1-8
- Jain A, Lamark T, Sjøttem E, Bowitz Larsen K, Atesoh Awuh J, Øvervatn A, McMahon M, Hayes JD, Johansen T (2010) p62/SQSTM1 Is a Target Gene for Transcription Factor NRF2 and Creates a Positive Feedback Loop by Inducing Antioxidant Response Element-driven Gene Transcription. *Journal of Biological Chemistry* 285:22576-22591
- Kageyama S, Saito T, Obata M, Koide RH, Ichimura Y, Komatsu M (2018) Negative Regulation of the Keap1-Nrf2 Pathway by a p62/Sqstm1 Splicing Variant. *Mol Cell Biol* 38
- Katsuragi Y, Ichimura Y, Komatsu M (2015) p62/SQSTM1 functions as a signaling hub and an autophagy adaptor. *FEBS Journal* 282:4672-4678
- Kim S, Ho Hur J, Park C, Kim H, Oh G, Lee JN, Yoo S, Choe S, So H, Lim DJ, Moon SK, Park R (2015) Bucillamine prevents cisplatin-induced ototoxicity through induction of glutathione and antioxidant genes. *Experimental & Molecular Medicine* 47:e142-e142
- Kobayashi A, Kang M, Okawa H, Ohtsuji M, Zenke Y, Chiba T, Igarashi K, Yamamoto M (2004) Oxidative Stress Sensor Keap1 Functions as an Adaptor for Cul3-Based E3 Ligase To Regulate Proteasomal Degradation of Nrf2. *Molecular and Cellular Biology* 24:7130-7139
- Komatsu M, Kurokawa H, Waguri S, Taguchi K, Kobayashi A, Ichimura Y, Sou Y, Ueno I, Sakamoto A, Tong KI, Kim M, Nishito Y, Iemura S, Natsume T, Ueno T, Kominami E, Motohashi H, Tanaka K, Yamamoto M (2010) The selective autophagy substrate p62 activates the stress responsive transcription factor Nrf2 through inactivation of Keap1. *Nature Cell Biology* 12:213-223
- Kong L, Chen G, Zhou X, McGinnis JF, Li F, Cao W (2009) Molecular mechanisms underlying cochlear degeneration in the tubby mouse and the therapeutic effect of sulforaphane. *Neurochemistry International* 54:172-179
- Lau A, Wang X, Zhao F, Villeneuve NF, Wu T, Jiang T, Sun Z, White E, Zhang DD (2010) A Noncanonical Mechanism of Nrf2 Activation by Autophagy Deficiency: Direct Interaction between Keap1 and p62. *Molecular and Cellular Biology* 30:3275-3285
- Lee D, Ko W, Song B, Son I, Kim D, Kang D, Lee H, Oh H, Jang J, Kim Y, Kim S (2016) The herbal extract KCHO-1 exerts a neuroprotective effect by ameliorating oxidative stress via heme oxygenase-1 upregulation. *Molecular Medicine Reports* 13:4911-4919

Li P, Bing D, Wang S, Chen J, Du Z, Sun Y, Qi F, Zhang Y, Chu H (2019) Sleep Deprivation Modifies Noise-Induced Cochlear Injury Related to the Stress Hormone and Autophagy in Female Mice. *Frontiers in Neuroscience* 13

Liu W, Xu Z, Yang T, Deng Y, Xu B, Feng S, Li Y (2014) The protective role of tea polyphenols against methylmercury-induced neurotoxic effects in rat cerebral cortex via inhibition of oxidative stress. *Free Radical Research* 48:849-863

Menardo J, Tang Y, Ladrech S, Lenoir M, Casas F, Michel C, Bourien J, Ruel J, Rebillard G, Maurice T, Puel J, Wang J (2012) Oxidative Stress, Inflammation, and Autophagic Stress as the Key Mechanisms of Premature Age-Related Hearing Loss in SAMP8 Mouse Cochlea. *Antioxidants & Redox Signaling* 16:263-274

Pan J, Sun Y, Jiang Y, Bott AJ, Jaber N, Dou Z, Yang B, Chen J, Catanzaro JM, Du C, Ding W, Diaz-Meco MT, Moscat J, Ozato K, Lin RZ, Zong W (2016) TRIM21 Ubiquitylates SQSTM1/p62 and Suppresses Protein Sequestration to Regulate Redox Homeostasis. *Molecular Cell* 61:720-733

Rogov V, Dotsch V, Johansen T, Kirkin V (2014) Interactions between autophagy receptors and ubiquitin-like proteins form the molecular basis for selective autophagy. *Mol Cell* 53:167-78

Wang B, Cao P, Wang Z, Li Z, Wang Z, Ma J, Liao B, Deng Y, Long X, Xu K, Wang H, Wang H, Zeng M, Lu X, Liu Z (2017) Interferon- $\gamma$ -induced insufficient autophagy contributes to p62-dependent apoptosis of epithelial cells in chronic rhinosinusitis with nasal polyps. *Allergy* 72:1384-1397

Wilson MI, Gill DJ, Perisic O, Quinn MT, Williams RL (2003) PB1 domain-mediated heterodimerization in NADPH oxidase and signaling complexes of atypical protein kinase C with Par6 and p62. *Mol Cell* 12:39-50

Wu F, Xiong H, Sha S (2020) Noise-induced loss of sensory hair cells is mediated by ROS/AMPK $\alpha$  pathway. *Redox Biology* 29:101406

Xiong H, Chen S, Lai L, Yang H, Xu Y, Pang J, Su Z, Lin H, Zheng Y (2019) Modulation of miR-34a/SIRT1 signaling protects cochlear hair cells against oxidative stress and delays age-related hearing loss through coordinated regulation of mitophagy and mitochondrial biogenesis. *Neurobiology of Aging* 79:30-42

## Figures

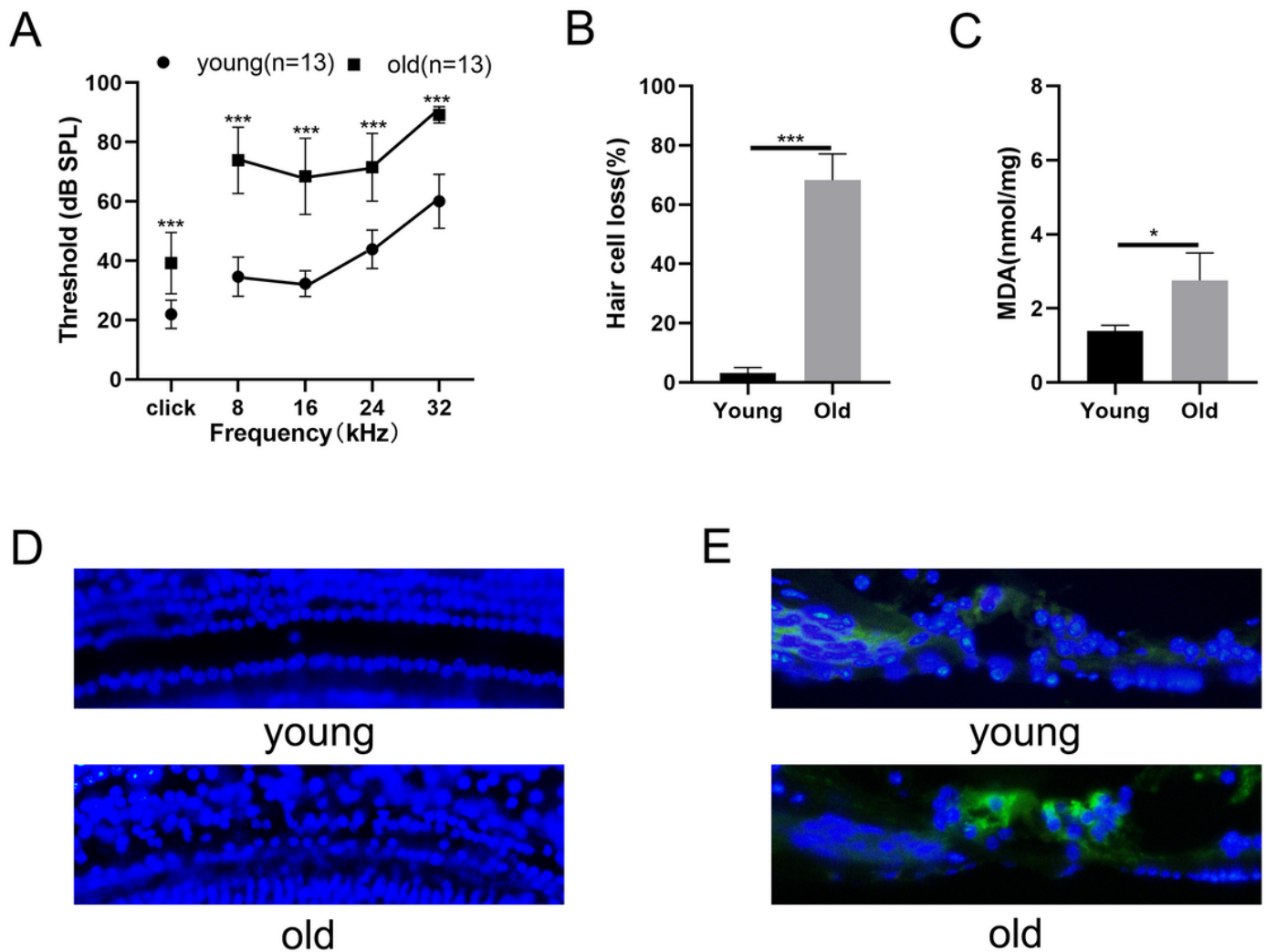


**Figure 1**

Audiometric threshold, hair cells (HCs), malondialdehyde (MDA) levels and 7, 8-dihydro-8-oxoguanine (8-oxoG) expression in young and old mice. (A) Mean  $\pm$  SD. Audiometric threshold (dB) determined from click and pure tone evoked ABRs. The threshold was significantly different between young mice and old mice (Student's t-test, click:  $P < 0.001$ , 8 kHz:  $P < 0.001$ , 16 kHz:  $P < 0.001$ , 24 kHz:  $P < 0.001$ , 32 kHz:  $P < 0.001$ ) ( $n = 13$  mice per group). (B) Mean  $\pm$  SD. HC loss percentage in the basal cochlear turns. Significant differences were observed between young and old mice (Student's t-test,  $P < 0.001$ ) ( $n = 3$  mice per group). (C) Mean  $\pm$  SD. MDA level in the cochleae. The levels of old mice were significantly higher than those of the young mice (Student's t-test,  $P = 0.034$ ). The experiment was repeated three times. (D) DAPI labeling of HCs nucleus (blue) in the basal turn. (E) Fluorescence immunohistochemistry of 8-oxoG in cochlear basilar membrane ( $n = 3$  mice per group).

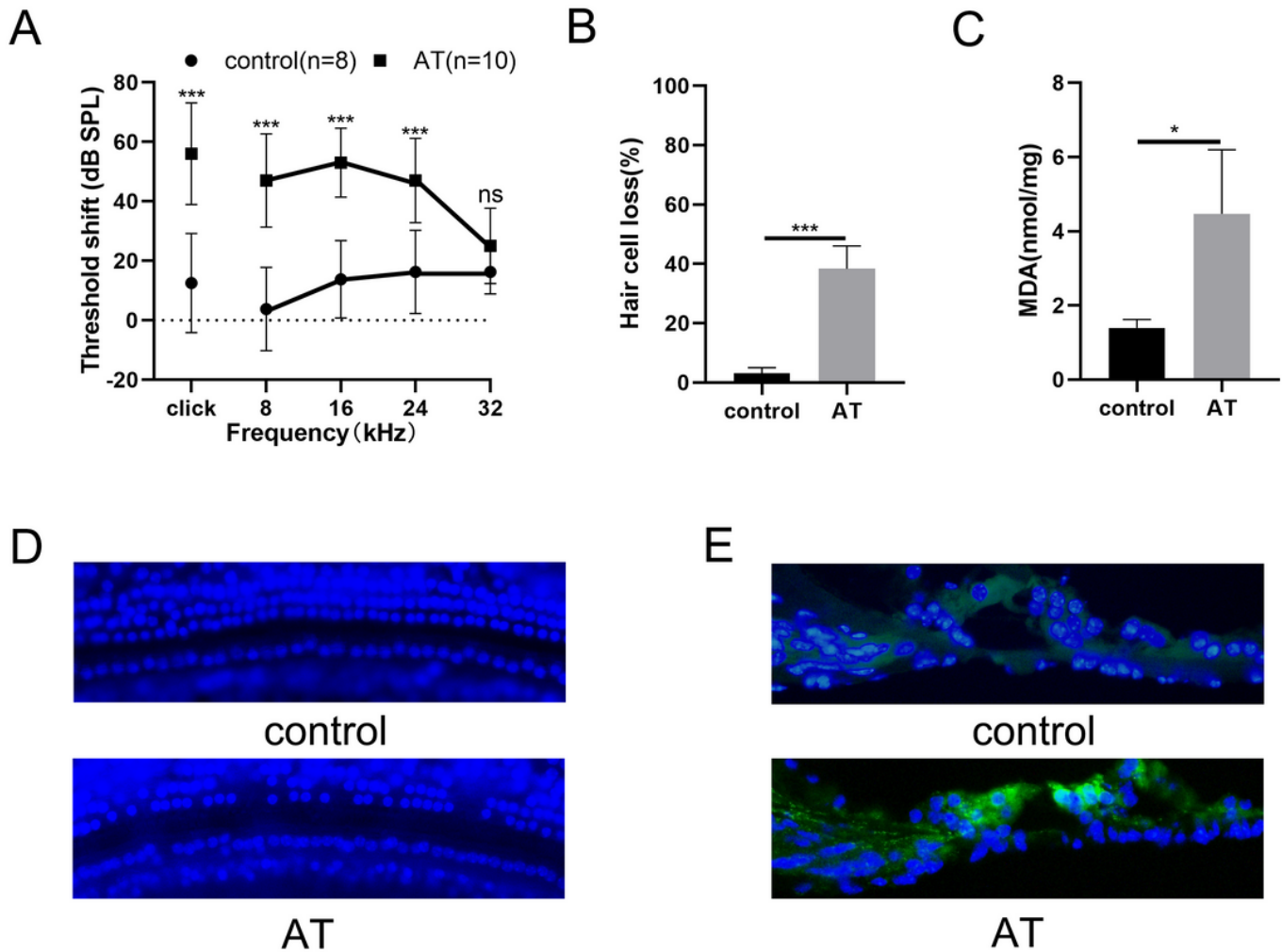


**Figure 2**

Audiometric threshold, hair cells (HCs), malondialdehyde (MDA) levels and 7, 8-dihydro-8-oxoguanine (8-oxoG) expression for control and AT groups. (A) Mean  $\pm$  SD. Audiometric threshold (dB) determined from click and pure tone evoked ABRs. The threshold was significantly different between control and AT mice for click ( $P < 0.001$ ), 8 kHz ( $P < 0.001$ ), 16 kHz ( $P < 0.001$ ) and 24 kHz ( $P < 0.001$ ). No significant difference was observed for 32 kHz ( $P = 0.104$ ) (control group:  $n = 8$ , AT group:  $n = 10$ ). Differences were compared using the Student's t-test. (B) Mean  $\pm$  SD. HC loss percentage in the basal cochlear turns. Significant differences were observed between control and AT groups (Student's t-test,  $P < 0.001$ ) ( $n = 3$  mice per group). (C) Mean  $\pm$  SD. MDA levels in the cochleae. The levels in the AT mice were significantly higher than those of control mice (Student's t-test,  $P = 0.038$ ). The experiment was repeated three times. (D) DAPI labeling of HC nucleus (blue) in the basal turn. (E) Fluorescence immunohistochemistry of 8-oxoG in cochlear basal membrane ( $n = 3$  mice per group).

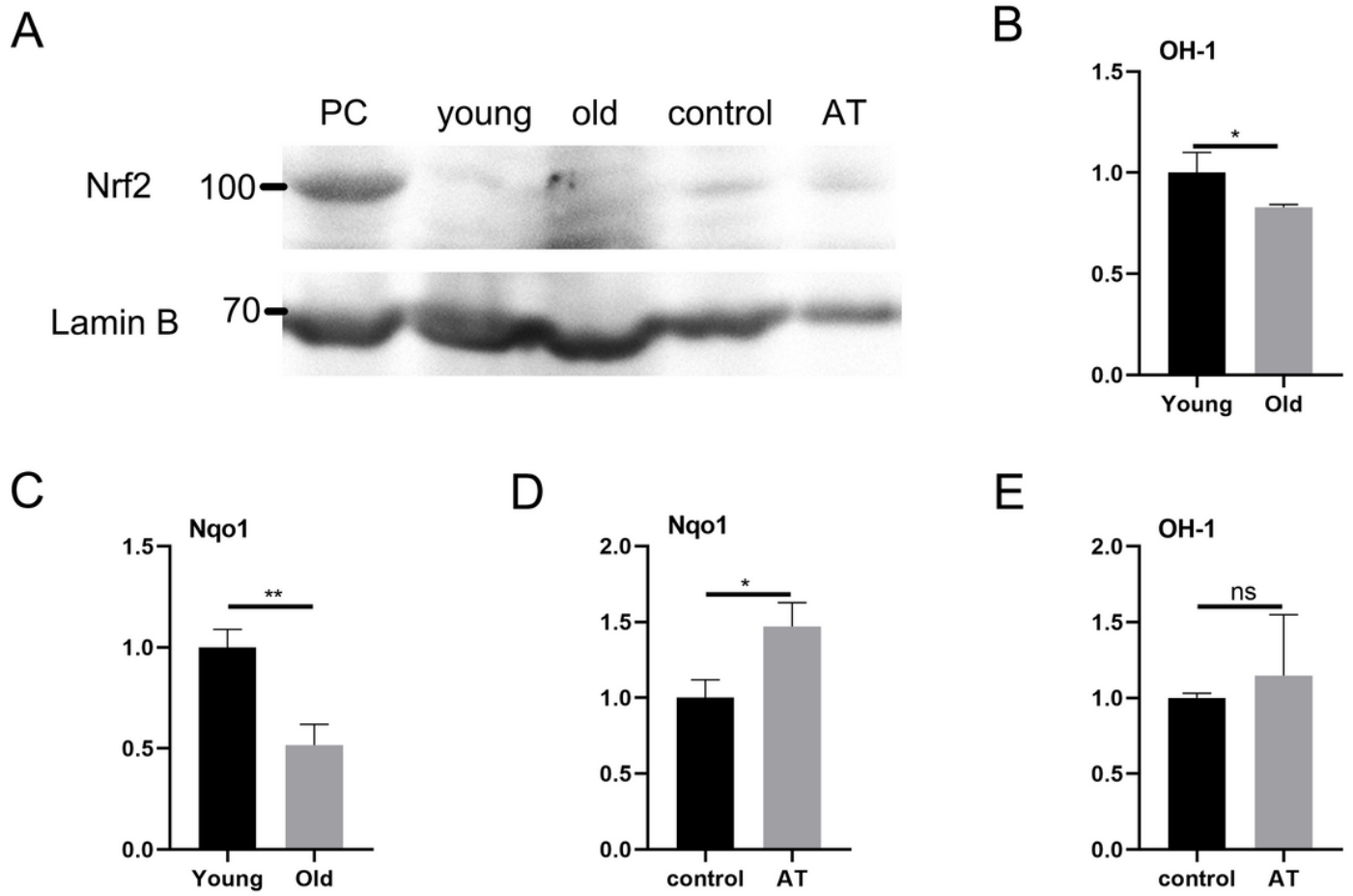


**Figure 3**

Nrf2 nuclear translocation and HO-1/NQO-1 mRNA expression. (A) The immunoblot of Nrf2 showed no obvious changes in nuclear protein during aging and overexposure. (B) HO-1 mRNA expression for young mice and old mice. (C) NQO-1 mRNA expression for young and old mice. (D) HO-1 mRNA expression for control and AT groups. (E) NQO-1 mRNA expression for control and AT group. Each experiment was repeated at least three times. The data are shown as mean  $\pm$  SD. Two-tailed, unpaired Student's t-tests were used to determine statistical significance.

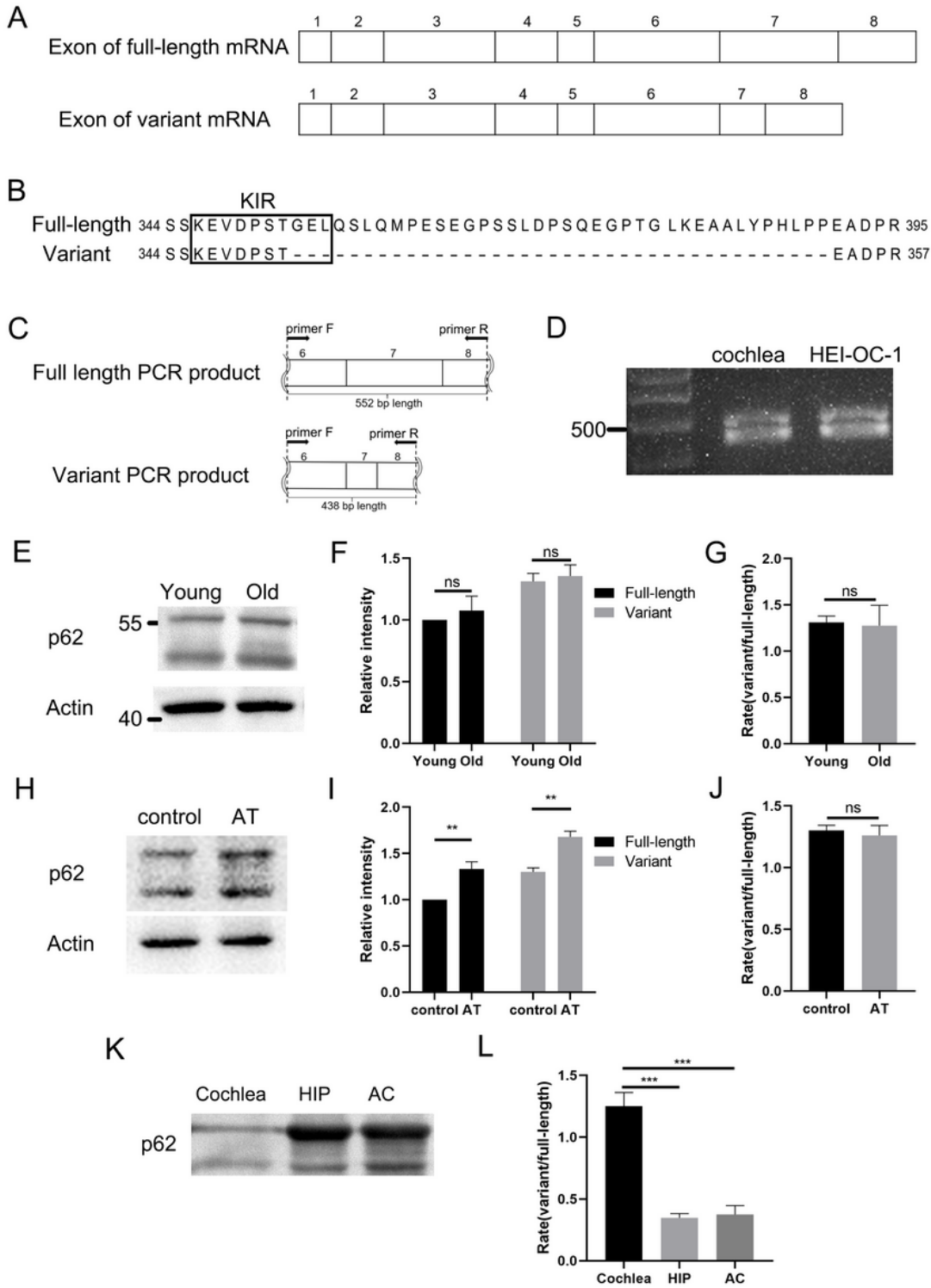


**Figure 4**

The exon of mRNA sequences and protein expression for full-length and splice variant p62. (A) The exon of mRNA sequences for full-length and splice variant p62. The variant p62 mRNA lacks the last half of exon 7. (B) The KIR region in the full-length and variant p62 proteins. (C) The qRT-PCR primers for identifying mRNA sequences of the full-length and splice variant p62. (D) Gel electrophoresis of RT-PCR products from cDNAs of cochleae and HEI-OC-1 cells. (E) The immunoblot of p62 for young and old mice.

(F, G) The analysis of (E). (H) The immunoblot of p62 for control and AT group. (I, J) The analysis of (H). (K) The immunoblot of p62 for cochlea, hippocampus (HIP), and auditory cortex (AC). (L) The analysis of Figure 4K. Each experiment was repeated at least three times. The data are shown as mean  $\pm$  SD. Two-tailed, unpaired Student's t-tests were used to determine statistical significance.

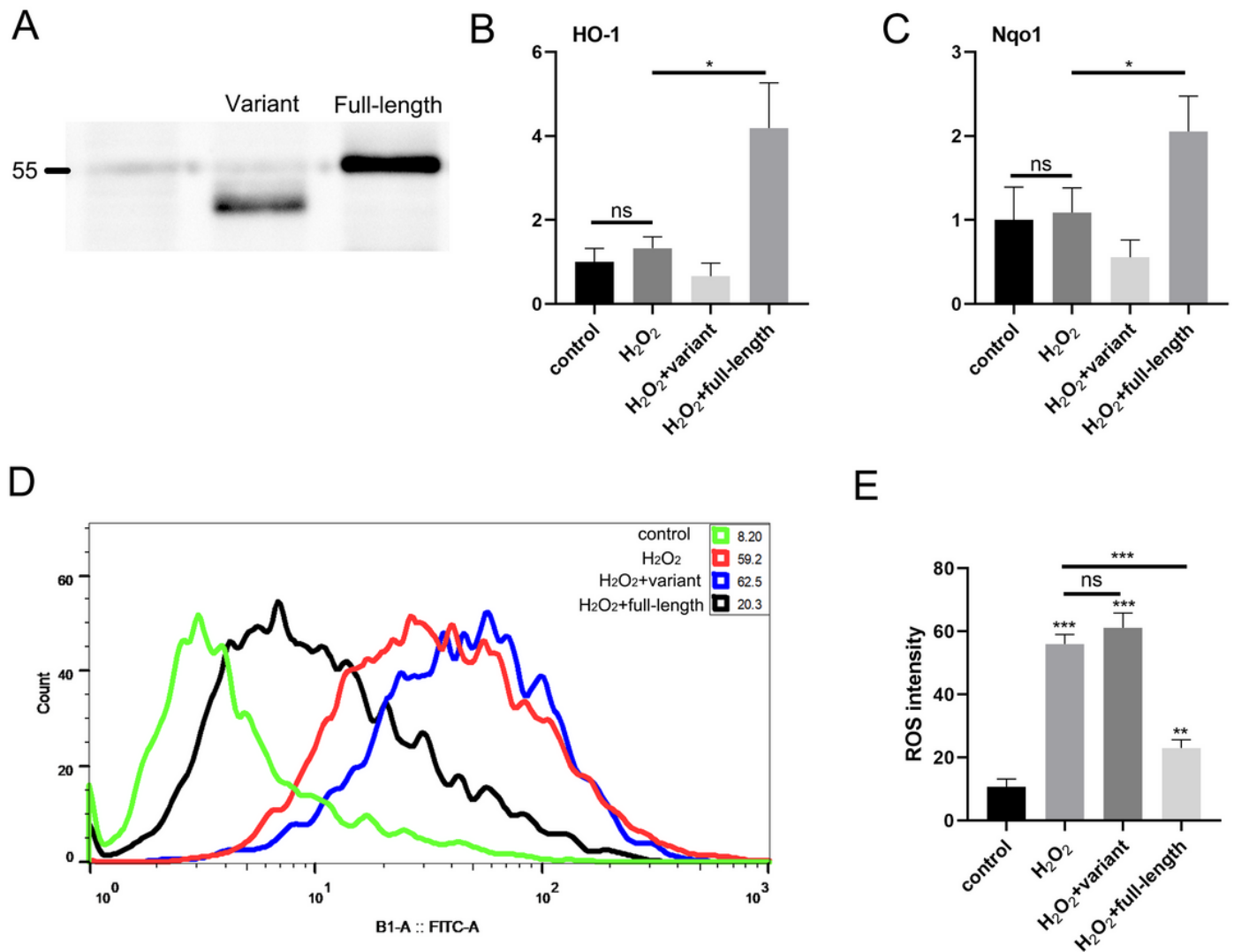


**Figure 5**

The HO-1/NQO-1 mRNA expression and the ROS levels in HEI-OC-1 cells. (A) The immunoblot of flag for the overexpressing FLAG-tagged full-length p62 and its variant groups. (B, C) HO-1/NQO-1 mRNA expression in cells. (D) ROS levels in HEI-OC-1 cells. (E) The analysis of (D). Each experiment was repeated at least three times. The data are shown as mean  $\pm$  SD. Two-tailed, unpaired Student's t-tests were used to determine statistical significance.